Journal of Hydrology 604 (2022) 127250

Contents lists available at ScienceDirect

Journal of Hydrology

journal homepage: www.elsevier.com/locate/jhydrol

Research papers

Hydrogeochemical changes before and during the 2019 Benevento seismic swarm in central-southern Italy

Francesca Gori, Marino Domenico Barberio *

[1] *Department of Earth Sciences, Sapienza University of Rome, Italy*

ARTICLE INFO

This manuscript was handled by Corrado Corradini, Editor-in-Chief, with the assistance of Carla Saltalippi, Associate Editor.

Keywords:
Hydrogeochemistry
Earthquakes
Hydrosensitivity
Carbon dioxide
Groundwater mixing
Deep fluids

ABSTRACT

Insights into seismic precursors have been obtained in the last decades. However, a detailed understanding of hydrogeochemical anomalies prior to earthquakes still remains the aim of many research teams worldwide. In order to investigate the earthquake-groundwater relationship, between 2018 and 2020, we performed sampling surveys coupled with continuous multiparametric monitoring in Grassano spring fed by the Matese aquifer (central-southern Apennines, Italy). Hydrogeochemical changes were observed before the onset and during the 2019 Benevento seismic sequence, including dissolved CO_2 increase, pH lowering, and anomalies in major ions (i.e., Ca^{2+}, Na^{+}, HCO_3^{-}) that later recovered to their typical concentrations. We suggest that variations in groundwater geochemistry were induced by dilatative preparatory phases of earthquakes, typical of the extensional setting. This condition allowed the deep CO_2 upwelling along tectonic discontinuities, as testified by the C_{ext} (carbon from external sources) behaviour detected in Grassano groundwater during the 2019 year. Despite the small-intermediate magnitude of the mainshock, results highlight and confirm the occurrence of a potential pre-seismic geochemical process in the fractured carbonate aquifers, similar to the one proposed in literature for the stronger 2016–2017 Amatrice-Norcia seismic sequence.

1. Introduction

Detecting earthquake precursors is one of the most compelling challenges in Earth sciences. Groundwater changes induced by seismic activity have been widely documented all over the world (Wakita, 1975; Muir-Wood and King, 1993; Elkhoury et al., 2006; Manga and Wang, 2015). Many studies shed light on the variation of crustal fluids behaviour after the occurrence of seismic events. However, in the last decades attempts to identify preseismic anomalies have been carried out too (Wakita et al., 1980; Igarashi et al., 1995; Salazar et al., 2002; Ingebritsen and Manga, 2014; Chen et al., 2015). In detail, changes in spring discharge (Petitta et al., 2018; Mastrorillo et al., 2020), groundwater level (Kim et al., 2019; Hwang et al., 2020; Lan et al., 2021), geochemical content (Kim et al., 2020; Nakagawa et al., 2020), isotope composition (Skelton et al., 2014; Onda et al., 2018; Hosono et al., 2020), dissolved and free gases (Pérez et al., 2006; Sano et al., 2016; Kawabata et al., 2020) have been recognized. Several study cases are from China, Japan, Italy, Iceland, and Korea where the set-up of hydrogeochemical networks has been already established or is currently in progress (Shi et al., 2013; Orihara et al., 2014; Andrén et al., 2016; Barberio et al., 2017; De Luca et al., 2018; Skelton et al., 2019; Li et al., 2019; Hosono and Masaki, 2020; Martinelli et al., 2021; Barbieri et al., 2021; Lee et al., 2021). Most of the interpretations agree in attributing hydrogeochemical anomalies to groundwater mixing between different aquifers driven by crustal dilation prior to seismic events (Tsunogai and Wakita, 1995; Claesson et al., 2004; Doglioni et al., 2014; Skelton et al., 2014; Andrén et al., 2016). In order to deepen understanding of the groundwater-earthquake relationship, related geochemical models have been also developed (Wästeby et al., 2014; Boschetti et al., 2019). Despite these scientific efforts, the knowledge about hydrogeochemical behaviour related to the seismic cycle need more observations to carry out a statistical analysis aimed at identifying a common denominator. In particular, the three main questions that are searching for answers are: When, Where and How the next earthquakes will occur. To achieve this objective, several study cases are necessary to build up appropriate geochemical models, naturally associated with different geo-tectonic contexts. This goal can be reached only through the increase of observations that can help to provide useful constraints on models (Wang and Manga, 2021).

Towards this direction, since 2014, a multiparametric monitoring

* Corresponding author at: Earth Sciences Department, Sapienza University of Rome, Piazzale Aldo Moro, 5, Rome, Italy.
E-mail address: marinodomenico.barberio@uniroma1.it (M.D. Barberio).

https://doi.org/10.1016/j.jhydrol.2021.127250
Received 28 July 2021; Received in revised form 19 November 2021; Accepted 21 November 2021
Available online 26 November 2021

network (consisting of two monitoring sites i.e., Sulmona and Matese areas) has been developed in central Italy by our research group, with the main aim of identifying preseismic signals in groundwater (Barberio et al., 2017; Boschetti et al., 2019; Barbieri et al., 2020; Barberio et al., 2020; Franchini et al., 2021; Coppola et al., 2021).

This study had two main objectives: identifying hydrogeochemical changes related to seismicity and putting them in a conceptual geochemical model. Additionally, we tried to achieve these purposes even for small-intermediate earthquake magnitudes ($M_w < 5$). We reported new hydrogeochemical changes induced by the 2019 Benevento seismic swarm (main earthquake: M_w 3.9) recorded in the Matese Node (i.e., Grassano spring). In detail, we measured variations in pH, CO_2, electrical conductivity, and some major elements before and in conjunction with the onset of the seismic swarm. The temporal sequence of hydrogeochemical recorded changes allows us to recognize the potential geochemical mechanism that triggered anomalies as discussed about the 2016–2017 Amatrice-Norcia seismic sequence (main earthquake M_w 6.5; Boschetti et al., 2019). This relationship is surprising and constitutes a novelty, since most of the research on this topic detected geochemical changes only for mainshock stronger than 5 (Inan et al., 2012; Skelton et al., 2014).

We are confident that findings can help geoscientist to better understand the hydrogeochemical responses of shallow aquifer system to deep fluid injection in different geological context (e.g., both seismic and volcanic areas; Amonte et al., 2021; Barbieri et al., 2021).

2. Geological and hydrogeological setting

The central-southern Apennines fold-and-thrust belt developed during Neogene and Quaternary times (Doglioni et al., 1996). The orogenesis is related to the W-dipping subduction of the Apulian lithosphere, whose slab retreat caused the progressive eastward migration of the foreland flexure, thrust fronts, and of the extensional back-arc tectonics (Doglioni, 1991; Cardello et al., 2021). The chain is characterized by NE-verging thrust faults, which dissected the tectonic edifice into several thick tectonic sheets. Since the Late Miocene, the post-orogenic crustal extension has affected the Apennines from west to east, forming half-graben intramountain basins, controlled by high-angle W-dipping normal faults and mostly filled by Pliocene-Quaternary continental deposits (Cavinato and Celles, 1999). At present times, the extensional tectonics is still ongoing, and it is currently strongly seismogenic along the axial region of the Apennines, whereas compressive kinematics is active in the Adriatic front, consistently with the regional stress field (Galli et al., 2008). The main domain is represented by the Meso-Cenozoic carbonate units, formed by limestone, dolomitic limestone, and dolomitic series of carbonate platform facies. The wide carbonate ridges of central-southern Apennines can store huge volumes of groundwater, acting as the main aquifer systems. Their hydrogeological complexity is essentially defined by the high transmissivity due to fracturing and locally karstification. Generally, groundwater is drained by large discharge springs with steady flow rate at the boundaries of the aquifers, where carbonate rocks are in contact with low-permeability deposits (aquicludes or aquitards), such as pre- and *syn*-orogenic basinal and flysch clayey series (Allocca et al., 2014).

In detail, the wide karst area of the Matese Massif, about 1500 km^2, crops out in the median sector of the Apennine chain, with elevations up to 2050 m (Fiorillo and Pagnozzi, 2015; Rufino et al., 2021). The main lithological units are the Late Triassic-Miocene carbonate sequences (i.e., limestones and dolostone) which reach thickness ranging between 2500 and 3000 m and are heavily fractured and faulted (Fiorillo and Guadagno, 2010; Silverii, 2016). From a seismological point of view, this area is considered one of the most active sectors of the Apennines, characterized by the presence of two main fault systems: one within the core of the massif, i.e., fault system of Matese-Gallo-Letino lakes (MGLF) and the Aquae Iuliae normal fault (AIF), and a second one at its western side i.e., the Ailano-Piedimonte Matese normal faults, (AIPMF) (Boncio et al., 2016).

The basal groundwater flowpath of the Matese aquifer is constrained by tectonic discontinuities, as well as geometric relationships between stratigraphical units (Celico and Petrella, 2008; Fiorillo et al., 2019; Rufino et al., 2021). Along the northern and eastern sectors, the Matese massif is tectonically joined by a thrust fault to low permeability argillaceous complexes and flysch sequences (Petrella and Celico, 2009). Instead, along the southern and western sectors, it is bounded by normal faults and covered by recent Quaternary deposits of the Volturno river plain. The Matese massif is characterized by many endorheic areas located at high elevations, whose formation is associated with the upper Pliocene-Pleistocene tectonic activity. These areas play a crucial role in recharge processes. Particularly, the Lago Matese polje represents the main recharge zone of the aquifer, occupying an area of 45 km^2 between 1000 and 2050 m a.s.l. (Fiorillo and Pagnozzi, 2015). Grassano-Telese springs are fed by the eastern sector of the Matese aquifer which is hydraulically connected by buried karst terrains and outcropping karst reliefs as Mt. Monaco, Mt. Acero, and Montepugliano (Fig. 1. Montepugliano relief is the discharge zone of a wide portion of the Matese aquifer, where a deep and wide groundwater circulation locally converge providing a general upwelling flow, driven by conduits and fracture networks (Fiorillo et al., 2019). Indeed, among the three main spring groups, Grassano-Telese springs, located at the southern slope of Montepugliano relief, represent the main discharge zone of the aquifer and the lowest elevation outflows (54 m a.s.l.) (Leone et al., 2019). These springs are characterized by both cold calcium-bicarbonate waters (Grassano spring) and hypothermal sulphurous and CO_2-rich ones (Telese spring) (Corniello and De Riso, 1986; Fiorillo et al., 2019). Grassano spring consists of different outlets with a mean annual discharge of 4.5 m^3/s, while the average discharge of Telese spring is about 1 m^3/s (Corniello et al., 2021). Besides, the isotopic signature of these springs reveals the same catchment area. Therefore, mineralization occurs in the final part of the groundwater flowpath, where uprising of deep gases (CO_2 and H_2S) occurs along the faults of Montepugliano relief (Corniello et al., 2021).

3. Material and methods

In this study, we analysed hydrogeochemical, gas-geochemical, isotopic and seismic data in order to investigate earthquake-induced effects on groundwater. Between February 2018 to September 2020, we performed twenty sampling campaigns at Grassano spring (Lat. 41.225040°, Long. 14.514426°, altitude 54 m) to look into groundwater hydrogeochemistry. Additionally, we carried out sampling at Telese spring (Lat. 41.223350°, Long. 14.525977°, altitude 57 m) and specifically, in June 2020 we executed a sampling survey addressed to collect data useful for the calculation of the groundwater carbon mass balance (e.g., major ions, chemical-physical parameter and isotope composition of CO_2).

In detail, chemical-physical parameters were measured on-site through the multiparametric probe WTW Multi 3420: temperature (resolution 0.1 °C), pH (resolution 0.001), and electrical conductivity (EC). Standard analytical methods were applied to characterize the chemical composition (Bridgewater et al., 2017). For the determination of major (anions and cations) elements, groundwater samples (filtered in situ through a 0.45 μm filter) were collected into polyethylene bottles. Firstly, they were kept at low temperature in ice-filled fridge boxes to avoid alterations of water components, and then they were analyzed by ion chromatography at the Geochemistry Laboratory of the Department of Earth Sciences at Sapienza University of Rome. Specifically, chromatographs Dionex ICS 5000 and Dionex ICS 1100 were used to determine the anionic content (F^-, Cl^-, SO_4^{2-}, and NO_3^-) and the cationic one (Ca^{2+}, Mg^{2+}, Na^+, and K^+), respectively. As testified by the cation–anion balance checked on each sample, the analytical error associated with these instruments was less than 5%. Alkalinity was measured on-site by titration with 0.05 N HCl solution and methyl-orange as indicator. Data

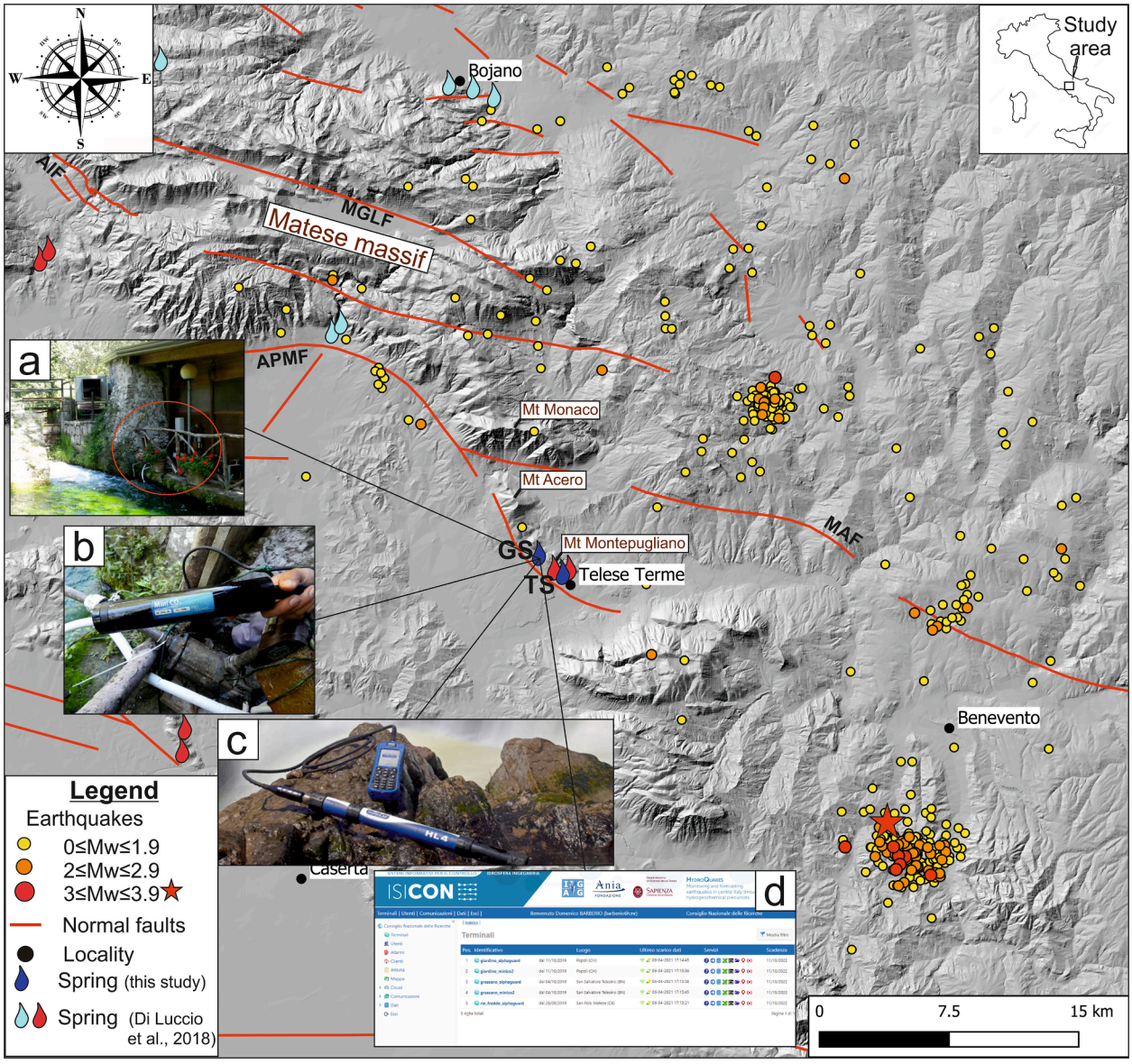

Fig. 1. Map of the study area (central-southern Apennines, see location in upper right inset). Active faults are from the Ithaca database (https://www.isprambiente.gov.it/en/projects/soil-and-territory/italy-hazards-from-capable-faulting). Base digital elevation model is from the ISPRA database SINAnet (https://www.sinanet.isprambiente.it/it). Locations of Grassano spring and Telese spring are displayed with blue drops and are reported as GS and TS, respectively. Springs (both of shallow, and hydrothermal systems, from Di Luccio et al., 2018), fed by the Matese aquifer and considered in the Result and Discussion section, are depicted with cyan and red drops, respectively. Earthquakes that occurred in the monitoring period (2018–2020) within a radial distance of 30 km from Telese Terme are shown with circles of different colors depending on the magnitude. The M_w 3.9 earthquake is displayed with a red star (http://terremoti.ingv.it/); Main faults are also displayed (MAF: Miranda Apice Fault, APMF: Ailano-Piedimonte Matese Fault; AIF: Aquae Iuliae Fault; MGLF: Matese-Gallo-Letino Fault). (a) Monitoring site; (b) MiniCO_2 probe for continuous monitoring of carbon dioxide; (c) HL4 probe for continuous monitoring of temperature, pH, and electrical conductivity, and dissolved oxygen; (d) Online system of data acquisition (https://webvision.digimatic.it/) used to investigate and download acquired time-series in real-time. (For interpretation of the references to colour in this figure legend, the reader is referred to the web version of this article.)

of major ions since February 13th, 2018 to January 8th, 2020 were also published in Franchini et al. (2021).

We performed continuous monitoring by installing two multiparametric probes (HL4 and Mini CO_2). The Hydrolab HL4 Multiparameter Probe measured continuously and simultaneously temperature, pH, and electrical conductivity, and dissolved oxygen. The device was equipped with integrated data recording capability. Measurements of parameters were automatically repeated and stored every 15 min, since July 19th, 2018 to October 29th, 2020. The Mini CO_2 Submersible Sensor (produced by Pro-Oceanus Systems Inc) was installed on May 24th, 2019, for the continuous monitoring of dissolved CO_2 concentrations. The gas was stripped from the water through a gas-permeable membrane and subsequently sent to the non-dispersive infrared detector (NDIR). With pCO_2 ranges from 0 to 10%, the instrument provided the versatility needed, by allowing the continuous acquisition of carbon dioxide concentrations, and repeating measurements every 15 min. Unfortunately, the firmware of the probe was damaged by a power surge on December 10th, 2019, therefore the sensor stopped acquiring data. Moreover, recorded data can be monitored and downloaded in real-time, by an online system of data acquisition developed by Digimatic s.r.l. (https://webvision.digimatic.it/).

Furthermore, thermodynamic calculations were carried out by using Phreeqc Interactive software for Windows (version 3), precisely the *prheeqc.dat* thermodynamic dataset (Parkhurst and Appelo, 2013).

Sample water conditions of T, pH, major ions, and alkalinity were used as input data to calculate the molality concentrations of the water content. In detail, the total molality of Ca, Mg, SO_4, and TDIC (mol/kg H_2O) was used for the calculation of C_{carb} and C_{ext} parameters in the following carbon mass balances (Chiodini et al., 2000):

$$TDIC=C_{carb}+C_{ext} \quad (1)$$

$$C_{carb}=Ca+Mg-SO_4 \quad (2)$$

$$C_{ext}=C_{TDIC}-C_{carb}=C_{inf}+C_{deep} \quad (3)$$

TDIC includes the total dissolved inorganic carbon in groundwater, whose origin is ascribable to the presence of different sources of carbon. Hence, it corresponds to the sum of these components (see Eq. 1). C_{carb} is the carbon derived from the water–rock interaction of groundwater with carbonate aquifers. Thus, the Eq. (2) considers the dissolution of calcite and dolomite, and also the presence of anhydrite and/or gypsum. C_{ext} is the carbon derived from "external sources", indeed it is expressed by the sum of two parameters (see Eq. 3): where C_{inf} is the carbon from atmospheric and biogenic CO_2 (i.e., the infiltrating waters), and C_{deep} is deep CO_2 from metamorphic, mantle, or magma sources (Chiodini et al., 2000; Chiodini et al., 2004).

The $\delta^{13}C$ isotope composition of deep CO_2 of Grassano spring was from Barbieri et al. (2020), while the one of Telese spring was obtained in this study. In detail, it was analysed by using a Thermo Scientific Delta V Plus isotope ratio mass spectrometer. The $\delta^{13}C$-CO_2 value is in terms of δ‰ units (expressed as V-PDB, Vienna Pee Dee Belemnite international standard), with analytical error of ± 0.15‰. Analytical devices were provided by the National Institute of Geophysics and Volcanology (INGV, Palermo, Italy).

Finally, we selected all earthquakes (~370) that occurred in the same period of the hydrogeochemical monitoring within a radial distance of 30 km from Telese Terme (Lat. 41.216729°, Long. 14.526261°). This area was selected according to the strain radius-epicentral distance relationship proposed by Dobrovolsky et al. (1979). Seismic data come from the database run by National Seismic Network (available on the website: http://terremoti.ingv.it/). The amount of energy released (E) was estimated from the earthquake magnitude M_w through the magnitude-energy relationship (see Eq. 4; Gutenberg, 1956):

$$Log\ E = 1.5 \times M_w + 11.8$$

4. Results and discussion

Collected data at Grassano spring refer both to continuous and discrete sampling, and are represented by chemical-physical parameters, major ions, and dissolved CO_2. We also considered seismic data. All discrete measurements are reported in the Table S1. In this section we present and discuss only the data that we considered relevant with respect to the aim of this work. Table 1 displays the maximum, average, and minimum values of all main parameters recorded during 2018–2020 monitoring.

The hydrogeochemical facies of Grassano spring is shown in the Piper diagram (Fig. 2a, by clear calcium-bicarbonate facies with minimal variations during the study period.

To better understand the geochemical features of the analysed groundwater, we considered data published in a previous study (Di Luccio et al., 2018). Grassano groundwater are located between two end-members represented by the shallow system and the hydrothermal one (depicted as the blue ellipse and the red one, respectively in Fig. 2b. This observation agrees with the results of a recent research (Corniello et al., 2021) which points out the mixing between shallow regional flowpath, coming from Matese carbonate aquifer (Fig. 1, and the deep mineralized and gas-rich groundwater upwelling along faults (e.g., Telese spring, Fig. 1.

Fig. 3 shows parameters having a potential correlation with seismic activity. In detail, we displayed the whole time series, both discrete and continuous of CO_2, pH, electrical conductivity, and Calcium (Ca^{2+}), Sodium (Na^+) and Alkalinity (HCO_3^-) concentrations. Other measured parameters (i.e., temperature) and ions did not show any potential evidence of relationship with seismicity, and for this reason, based on the main purpose of this work, they are not discussed but they are reported in the Table S1. Stream discharge of the spring was not recorded in this study.

Fig. 3b displays CO_2 time series recorded from May 24th, 2019 to December 10th, 2019, which was characterized by several lacks of data due to electrical interruption. Besides, it is noteworthy that such time series is shorter than other continuous data because the probe was installed in May 2019 and it turned off in December 2019 owing to sensor damage. The average value was 6.4%. In the first period (since June to September 2019) the CO_2 values recorded a general increase from 6.0% to 6.8%. Later the trend was approximately steady around 6.7%. Evident CO_2 spikes are clearly discernible and are attributable to instrumental noises. Fig. 3c includes continuous pH time series recorded from July 19th, 2018 to October 29th, 2020, with missing data from March 2020 to June 2020. In addition, discrete pH measurements recorded during our campaign surveys were reported with circles. During five surveys, we had some problems with pH sensor of the portable WTW Multi 3420 probe. Therefore, for these cases, we recalculated pH value through the arithmetic mean of daily continuous values provided by the HL4 probe. Direct and recalculated data were displayed with cyan and green circles, respectively (Fig. 3c. Both continuous and discrete average values were about equal to 7.0. The time series were quite steady within a minimum value of 6.8 and a maximum one of 7.3 during the monitoring period. Despite this limited range of variation (0.5), a notable decrease was recorded since August 2018 to October 2018 (about 0.25), followed by 2 months of instrumental noises owing to some problems of the setting station on-field. Since June 7th, 2019 to September 10th, 2019, the series was firstly characterized by a sharp decrease equal to 0.3 and a subsequent clear increase of 0.2. Fig. 3d contains the electrical conductivity time series, both discrete and continuous, with the same interval and inconsistences of pH series (e.g., setting of the station and data lack). Again, recorded spikes in the signal were attributable to instrumental noises. Continuous and discrete average values were 905 μS/cm and 901 μS/cm, respectively. The time series values were quite steady around the mean, however a visible increase of about 45 μS/cm was detected since November 20th, 2019 to January 9th, 2020. Finally, time series of Ca^{2+}, Na^+ and HCO_3^-, consisting of the surveys performed between February 2018 and September 2020, are plotted in Fig. 3e, 3f, and 3 g. The average values of the analysed major ions (mg/L) were 174.5, 16.6, and 658, respectively (Table 1. Statistical distribution of ions concentrations was analysed through box-and-whiskers plots (Fig. 4. The box, separated into two parts by the median, represents the interquartile range (first and third quartiles). The whiskers are limited by the interquartile range

Table 1
Maximum, average and minimum values of major ions and chemical-physical parameters.

	Ca	Mg	Na	K	Cl	SO4	HCO3	F	NO3	EC	T	pH
	mg/L	mg/L	mg/L	mg/L	mg/L	mg/L	mg/L	mg/L	mg/L	μS/cm	°C	
Max	198.3	30.4	20.0	3.0	31.5	10.2	751.3	0.4	4.7	973.0	12.3	7.1
Average	174.5	27.4	16.6	2.4	23.8	8.2	658.0	0.1	2.8	901.1	11.7	7.0
Min	164.5	19.1	14.7	1.3	18.9	7.0	604.1	0.1	1.9	869.0	11.2	6.8

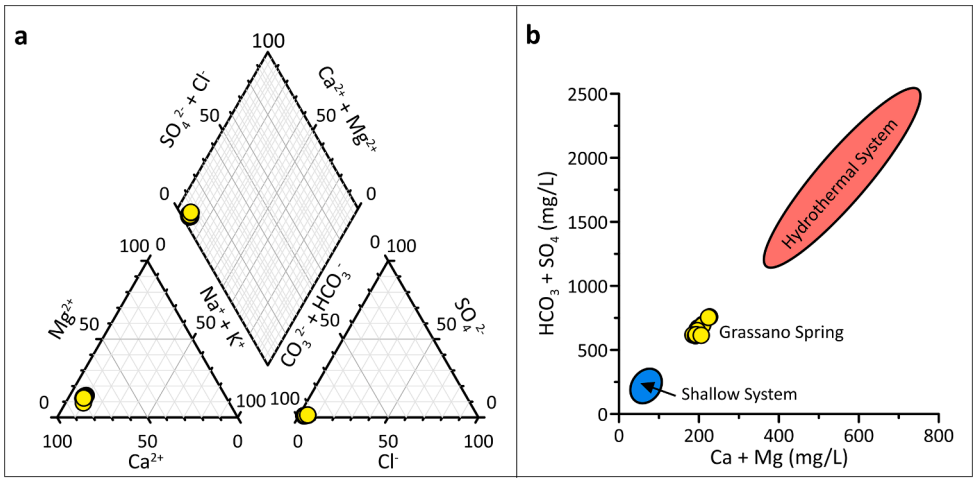

Fig. 2. (a) Piper diagram for the hydrogeochemical classification of groundwater samples, resulting enriched in bicarbonate and calcium ions (Ca-HCO_3 facies); (b) The major ion ratio (Ca + Mg/HCO_3 + SO_4) suggests that the hydrogeochemistry of Grassano spring (yellow circles) derives from the mixing between the shallow system (blue ellipse) and the hydrothermal one (red ellipse). Data of shallow and hydrothermal systems are from Di Luccio et al. (2018). (For interpretation of the references to colour in this figure legend, the reader is referred to the web version of this article.)

(IQR) with a factor equal to 1.5. This analysis revealed that all three ions were characterized by anomalous values (dots in Fig. 4 of concentrations (ppm) with respect to the whole distribution recorded in the three-years monitoring. Since "outliers" exceed the whiskers only in the surveys performed on November 19th, 2019, and on January 8th, 2020, they (and associated changes in electrical conductivity, pH values and dissolved CO_2) did not represent seasonal and/or natural hydrogeochemical variations.

During the monitoring period three main seismic sequences (see location in Fig. 1 and time series in Fig. 3a were clearly recognized among the typical background seismicity that characterized this sector of the Apennines (Milano et al., 2006). The first one was represented by 72 seismic events occurred since August 31st, 2018 to September 16th, 2018, about 15 km far from Grassano spring. The maximum earthquake had $M_w = 2.8$. The second, and the third seismic sequences occurred in the same area, about 25 km far from the monitoring site, near San Leucio del Sannio village. The first of these two sequences started on November 21st, 2019 and ended on December 17th, 2019. It included 87 seismic events and the maximum earthquake magnitude was equal to 3.9, recorded on December 16th, 2019. The same area was struck by a second and smaller swarm in March 2020, composed by 54 seismic events (maximum earthquake magnitude $M_w = 2.6$). The calculation of the Cumulated Energy (shown with the green line in Fig. 3a highlighted the strongest energy release in conjunction with the second seismic swarm.

Fig. 5 displays the time chart with the temporal sequence of significant detected variations. Changes in pH, electrical conductivity, and major ions concentrations are supposed to be related to the previously observed CO_2 increase in the aquifer system. To sum up, the CO_2 increase would induce a sudden pH decrease that was followed by a mild increase. In conjunction with the pH recovery to the previous values (e.g., values of May 2019), it was recorded an electrical conductivity increase coupled with anomalous high values of Ca^{2+}, Na^+, and HCO_3^- concentrations, exactly two days before the onset of the seismic sequence, and about one month before the main seismic event (i.e., the M_w 3.9 San Leucio del Sannio earthquake occurred on December 16th, 2019). However, discrete sampling did not allow to recognise exactly the moment in which concentrations of these ions started to increase. Anyway, this process was attributed to the reaction of the hosting aquifer system, the so-called "buffering effect" (Langmuir, 1997; Drever, 2005). In order to re-equilibrate the original chemical conditions after being hit by a CO_2 increase, the aquifer system naturally reacts through the following equations (Eq. 5, 6):

CO_2 (aq) + H_2O (aq) → H_2CO_3 → H^+ + HCO_3^- (induce pH decreasing) (5)

Dissolved HCO_3^- (groundwater) + H^+ (released) ⇄ H_2CO_3 (aq) (pH buffer) (6)

In detail, the addition of CO_2 to karst fractured carbonate aquifer dissolved both the carbonate fraction (Ca^{2+} and HCO_3^-) and weathered the silica one of the reservoir rocks (Minissale, 2004; Clark, 2015). Due to the buffering effect of the carbonate-bicarbonate (CO_3^{2-}– HCO_3^-) pair, the pH stabilizes when CO_2 is dissolved or exsolved (Amonte et al., 2021). Indeed, an ion exchange process could have involved the Na ions adsorbed onto clay minerals. In fact, cations have different tendencies to be adsorbed or desorbed. Their tendency for adsorption in natural waters is as follows: (strongly adsorbed) $Ca^{2+} > Mg^{2+} > K^+ > Na^+$ (weakly adsorbed), which means that sodium ions are much more likely to be desorbed from surfaces and then to be ejected and transferred into groundwater (Rajmohan and Elango, 2004; Manahan, 2017; Chen et al., 2021). Alternatively, such increase in Na concentrations could be just explained as deep fluid upwelling, in fact, high sodium concentration is certain feature of deeply originated fluids in deep reservoir in crust. Similar geochemical changes in groundwater were also recognized in other studies (Bourg and Loch, 1995; Malakootian and Nouri, 2010; Barberio et al., 2017; Paudel et al., 2018). For instance, the 2016–2017 Amatrice-Norcia seismic sequence, which occurred about 80 km far from the studied monitoring site, caused the CO_2 inflow in the shallow regional aquifer and consequently the pH variation, with consequent trace element mobilization (i.e., As, V, Cr, Fe; Barberio et al., 2017).

In addition, the geochemical modelling, conducted by Boschetti et al. (2019), confirmed that the variation in the CO_2 fugacity can change the adsorption/desorption process of some elements in the rock aquifer. In the present study, we suppose that a similar geochemical process could be inferred at Grassano spring. Indeed, Grassano spring is characterized by the presence of high dissolved CO_2 concentration, whose source is attributable to crustal deep degassing (Di Luccio et al., 2018). Hence, following previous studies (Frondini et al., 2019; Barbieri et al., 2020), a calculation of the carbon mass balance has been carried out to define the C_{ext} component useful to quantify and distinguish the carbon related to the deep source from the biogenic (C_{inf}) and carbonate (C_{carb}) ones.

Fig. 6a, shows the C_{ext} value versus the $\delta^{13}C_{ext}$ isotopic composition of Grassano spring (yellow circle), resulting between infiltrating waters (blue ellipse) and the CO_2 rich-springs (red rectangle) of the Matese aquifer. However, it is clear that the Grassano groundwater is closer to the deep end-member which corresponds to our sampling of Telese spring performed in June 2020 (red circle). Moreover, this evidence suggests the mixing between CO_2-rich deep groundwater, such as Telese spring, and Grassano spring that could be enhanced by dilatative preparatory phases of earthquakes, typical of the extensional setting (Sibson, 2000; Doglioni et al., 2014). Indeed, the $\delta^{13}C_{ext}$ isotopic ratio of Grassano spring is heavier compared to that of other carbonate springs of the Matese aquifer (data taken from Di Luccio et al., 2018), showing an endogenous signature (Barbieri et al., 2020). The contribution of

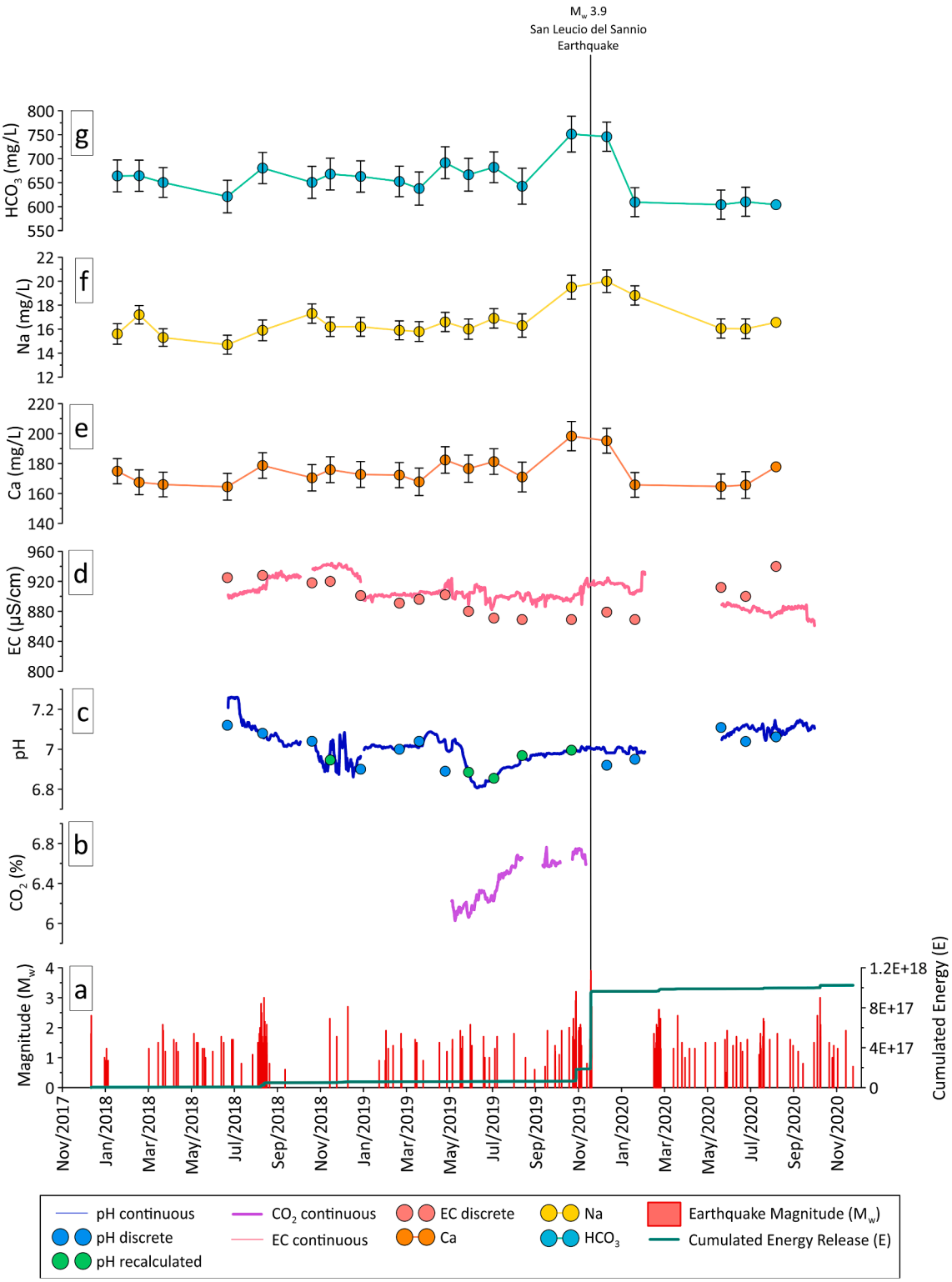

Fig. 3. (a) Time series (January 1st, 2018 – December 31st, 2020) of seismic activity: earthquakes occurred in the same period of the hydrogeochemical monitoring are shown with red bars, and the calculated cumulated energy release (Gutenberg, 1956) is displayed by a green line; Seismic data are from the INGV database (http://terremoti.ingv.it/); (b) Time series (May 24th, 2019 – December 10th, 2019) of CO_2 continuously recorded is shown by the purple line; (c) Time series (July 19th, 2018 – October 29th, 2020) of pH continuously recorded is shown with the blue line, while pH discrete sampling is displayed with cyan (direct measurements) and green (recalculated values) circles; (d) Time series (July 19th, 2018 – October 29th, 2020) of electrical conductivity both continuous and discrete are shown with pink line and circles, respectively; (e, f, g) Time series of major ions (i.e., Ca^{2+}, Na^{+}, and HCO_3^{-}), are shown with orange, yellow, and turquoise circles, respectively. (For interpretation of the references to colour in this figure legend, the reader is referred to the web version of this article.)

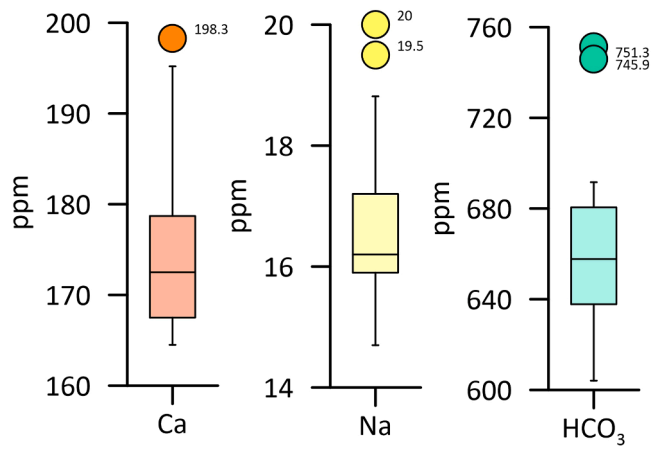

Fig. 4. Box-and-whiskers plots of major ions (Ca^{2+}, Na^{+}, and HCO_3^{-}) point out anomalous values (outliers) in November 2019 and January 2020.

deep CO_2 confirms the influence and the mixing with a deep circulation system, widely hidden by the large contribution to the discharge of the shallow carbonate circulation system. The calculation of the carbon mass balance of groundwater samples allows to obtain the C_{ext} time series shown in Fig. 6b. In detail, we recorded a progressive increase of C_{ext} through the entire 2019 year that reached the maximum value at the end of the seismic sequence, precisely in the survey performed in January 2020. The C_{ext} values of the last three surveys were among the minima measurements of the monitoring period. Also, pH, continuous electrical conductivity, major ions concentration recovered their preseismic values, consistently with our interpretation of geochemical processes.

We speculate that the increase of C_{ext} value during 2019 was due to deep pre-seismic geological processes (i.e., variation in dilation) that allowed the upwelling of the deep CO_2 flux along tectonic discontinuities. Through this multiparametric approach, it is possible to provide a description of a complex geochemical process that potentially induced the hydrogeochemical changes in Ca^{2+}, Na^{+}, and HCO_3^{-} just a few days before the onset of the seismic sequence. Apart from furnishing a potential hydrogeochemical model, it is also necessary to take a step forward to identify possible geo-structural mechanism that could induce the recorded geochemical responses.

It is noteworthy that fluids have an "active" role in decreasing fault strength, thereby they can influence fault mechanics, and the cyclic activation. Fluids can also act "passively" (e.g., Tullis et al., 1996; Wannamaker et al., 2002; Doglioni et al., 2014), being squeezed by pressure gradients, and transported depending on rock permeability (Salazar et a., 2002). Their migration, whatever the origin is (e.g., meteoric, crustal, or mantle-derived), is influenced by variation in the state of the stress. For example, as consequence of dilatancy and fluid-diffusion mechanism, fluids are rapidly redistributed in the crust (Sibson et al., 1975). Besides, also fluid discharges of opposite sign (i.e., negative and positive during the coseismic phase) have been documented along thrust and normal faults, respectively (Muir-Wood and King, 1993). Also, changes in hydrogeochemical content of groundwater may be expected because earthquake-induced groundwater flow is effective in transporting solutes, and seismic events may open new passageways to connect fluids from different reservoirs, and thus facilitating such exchange (Wang and Manga, 2021). Most variations in geochemical composition are consistent with the model of earthquake-

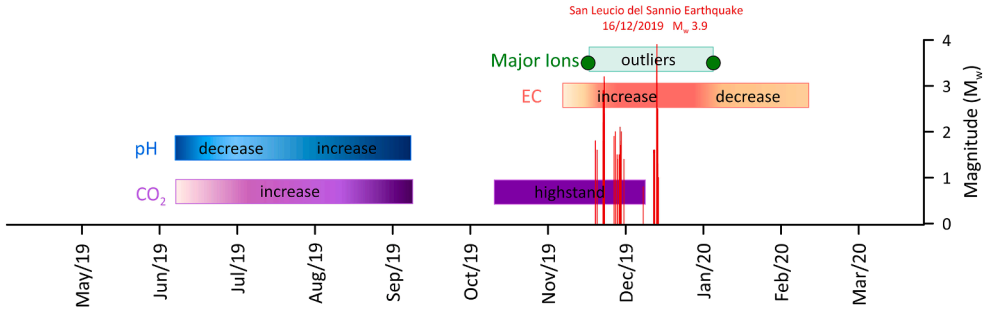

Fig. 5. Fig. 5. Time chart resuming the relevant hydrogeochemical variations. Outliers measured in major ions are depicted with two green points, while the horizontal light green bar shows the period in which we assume that concentration values presumably have remained high. (For interpretation of the references to colour in this figure legend, the reader is referred to the web version of this article.)

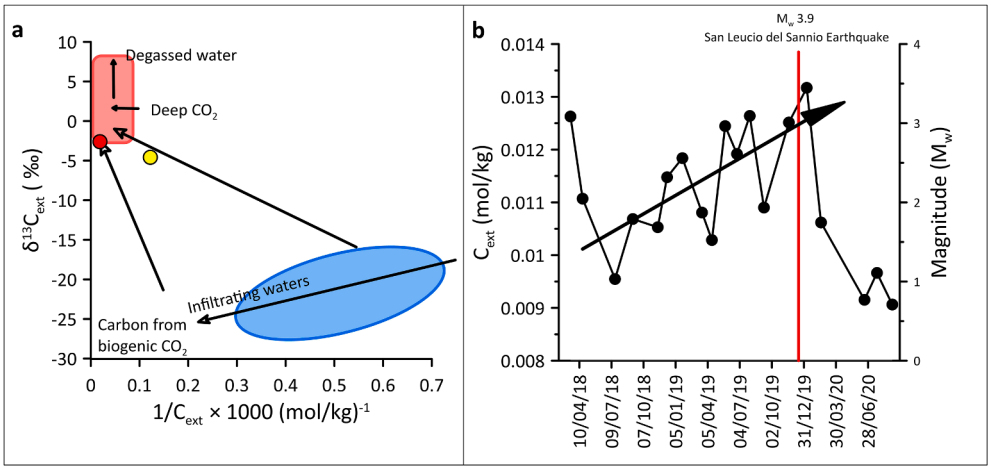

Fig. 6. (a) $\delta^{13}C_{ext}$ versus $1/C_{ext}$ diagram. Grassano spring is displayed with the yellow circle and Telese spring is represented by the red one. Data of other springs of the Matese carbonate aquifer (from Di Luccio et al., 2018) are displayed with the blue ellipse and the red rectangle, corresponding to infiltrating waters and to CO_2-rich springs, respectively. (b) Time series of C_{ext} (2018 – 2020) at Grassano springs calculated through the carbon mass balance (Chiodini et al., 2000). The M_w 3.9 mainshock is shown with a red bar. (For interpretation of the references to colour in this figure legend, the reader is referred to the web version of this article.)

enhanced groundwater transport through basin-wide or local enhanced permeability (Wang et al., 2013; Wang and Manga, 2021). It may breach hydrologic barriers (e.g., aquitards), connecting otherwise isolated aquifers or other fluid sources, and then causing fluid source switching and/or mixing (Wang and Manga, 2021). Studies of these processes can represent another step to improve the comprehension both about natural transport processes, and earthquake-induced hydrogeochemical responses. Despite data concerning hydrogeochemical changes are less abundant than those regarding changes in groundwater level and discharge, through the years they allowed to get useful information to constrain models of hydrogeological processes induced by seismicity (Wang and Manga, 2021).

According to a recent global analysis (Tamburello et al., 2018), there is a positive spatial correlation between CO_2 degassing and extensional tectonic regimes that would play a key role in creating pathways for the uprising deep fluids and connecting the deep portion of crust to the earth surface. Thus, normal faults, strike-slip faults and areas with high structural damage represent the most suitable scenario for CO_2 uprising (Lamberti et al., 2019). A widely accepted geo-structural model is based on the concept of stick–slip fault behaviour in the upper crust and on the presence of a stable sliding fault in the middle-lower crust (Doglioni et al., 2015; Petricca et al., 2015). The development of fault zone fracturing, together with hanging-wall dilation and initial collapse in the preseismic phase, produce high fluid pressure (e.g., CO_2), and consequently migration of fluids from the high pressure zone to the low pressure one (Doglioni et al., 2014).

During the 2019 Benevento seismic swarm, the seismicity delineated the existence of a subvertical WNW-ESE striking fault plane between 7 and 18 km depth. The estimated focal mechanism highlighted a right lateral strike-slip kinematics of the fault structure which accommodates differential extensional deformation and represents a potential source of $M_w > 5$ damaging earthquakes (Ciaccio et al., 2021). In this context, presumably, in the preseismic preparatory phase the deep fluids uprising in shallow regional aquifers could be enhanced due to the generation of high pore pressure along fault plane and fractures (Cardello and Mancktelow, 2015; Barberio et al., 2021).

Findings like those reported in our work are relevant because they confirmed, in similar geological and tectonic setting, a common geochemical process able to cause the same pattern of hydrogeochemical anomalies. In fact, we argue that the recorded geochemical responses were induced by a similar geochemical process that caused the anomalies prior to the 2016–2017 Amatrice-Norcia seismic sequence (main earthquake: M_w 6.5; Chiaraluce et al., 2017). The proposed tectonic model reconstructed for the two different study areas is the same too. Implications derived from our study can be applied to cases in other countries and in other geological contexts. For example, variations in groundwater hydrogeochemical content were also observed before and during volcanic activity in Iceland, and in Tenerife Island as consequence of pulses of fluid injection from volcanic and/or hydrothermal system (Barbieri et al., 2021; Amonte et al., 2021)

5. Conclusion

In this study, hydrogeochemical monitoring, both discrete and continuous, of chemical-physical parameters, major ions and dissolved CO_2 was performed in Grassano spring (central-southern Italy), with the aim of identifying in groundwater potential precursors of nearby earthquakes.

We conclude that:

- Anomalous concentrations of Ca^{2+}, Na^+ and HCO_3^- were recorded in one sample before and in another one after the 2019 Benevento seismic sequence (main earthquake on December 16th, 2019: M_w 3.9 San Leucio del Sannio).
- Changes in groundwater chemical content are attributable to the progressive increase of deep CO_2 in the aquifer system, which temporarily lowered pH and enhanced the solubility of the above-mentioned major ions.
- The deep pre-seismic dilatational processes are supposed to be responsible for enhancing the influx and ascent of CO_2 in the regional carbonate aquifer. In fact, the increase of CO_2 in the studied aquifer and spring started before the related seismic sequence.
- The geochemical process that occurred in Grassano groundwater prior to the seismic sequence was similar to that defined for the 2016–2017 Amatrice-Norcia seismic sequence, despite the seismicity during our monitoring period was characterized by small-intermediate magnitude.
- The obtained results shed light on the possibility of having pre-seismic hydrogeochemical signals in springs and groundwater also for small-intermediate earthquake magnitude, at least in the areas where deep fluids contribution to groundwater is evident.
- This study highlights also the crucial role of the multiparametric approach to expand the knowledge about the relationship between the geochemical process in groundwater and seismic activity. However, also other parameters as for example discharge rates as well as the groundwater level are needed to clarify some hydrogeological aspects.
- The setup of a standardized and diffuse monitoring network of groundwater, like that of this study, would produce significant and useful information towards the solving of the three main questions When, Where, and How the release of seismic energy will occur.

CRediT authorship contribution statement

Francesca Gori: Conceptualization, Methodology, Investigation, Formal analysis, Software, Data curation, Visualization, Writing – review & editing. **Marino Domenico Barberio:** Conceptualization, Methodology, Investigation, Formal analysis, Data curation, Software, Visualization, Writing – review & editing.

Declaration of Competing Interest

The authors declare that they have no known competing financial interests or personal relationships that could have appeared to influence the work reported in this paper.

Acknowledgements

We thank all our research team for the strong and enthusiastic support: Prof. Marco Petitta, Prof. Maurizio Barbieri, Dr. Andrea Billi, Prof. Tiziano Boschetti, Dr. Antonio Caracausi, Dr. Stefania Franchini, and Dr. Luca Pizzino. This study was partly funded by Fondazione ANIA (www.fondazioneania.it). We thank Dr. Umberto Guidoni (Fondazione ANIA), and his collaborators for granting the permit to publish these results. We acknowledge institutional financial support from Sapienza University of Rome, Italy (“Ateneo 2019” grant, title "Monitoraggio integrato delle acque sotterranee e sorgive dell’Appennino Centrale finalizzato alla verifica delle relazioni con la sismicità” P.I. Marco Petitta). We are also indebted to Prof. Carlo Doglioni (INGV and Sapienza University of Rome) who conceived, promoted, and supported the interdisciplinary researches on hydrogeochemical anomalies in seismic areas of Central Italy. Finally, we thank the Managers of Parco del Grassano and Telese Spa for allowing access and permitting to collect water samples.

Appendix A. Supplementary data

Supplementary data to this article can be found online at https://doi.org/10.1016/j.jhydrol.2021.127250.

References

Allocca, V., Manna, F., De Vita, P., 2014. Estimating annual groundwater recharge coefficient for karst aquifers of the southern Apennines (Italy). Hydrol. Earth Syst. Sci. 18, 803–817. https://doi.org/10.5194/hess-18-803-2014.

Amonte, C., Asensio-Ramos, M., Melián, G.V., Pérez, N.M., Padrón, E., Hernández, P.A., Rodríguez, F., D'Auria, L., López, D., 2021. Hydrogeochemical temporal variations related to changes of seismic activity at Tenerife, Canary Islands. Bull. Volcanol. 83 (4), 1–18.

Andrén, M., Stockmann, G., Skelton, A., Sturkell, E., Mörth, C.M., Guðrúnardóttir, H.R., Keller, N.S., Odling, N., Dahrén, B., Broman, C., Balic-Zunic, T., Hjartarson, H., Siegmund, H., Freund, F., Kockum, I., 2016. Coupling between mineral reactions, chemical changes in groundwater, and earthquakes in Iceland. J. Geophys. Res. Solid Earth 121 (4), 2315–2337.

Barberio, M.D., Barbieri, M., Billi, A., Doglioni, C., Petitta, M., 2017. Hydrogeochemical changes before and during the 2016 Amatrice-Norcia seismic sequence (central Italy). Sci. Rep. 7, 11735. https://doi.org/10.1038/s41598-017-11990-8.

Barberio, M.D., Gori, F., Barbieri, M., Billi, A., Caracausi, A., De Luca, G., Franchini, S., Petitta, M., Doglioni, C., 2020. New observations in Central Italy of groundwater responses to the worldwide seismicity. Sci. Rep. 10, 1–10.

Barberio, M.D., Gori, F., Barbieri, M., Boschetti, T., Caracausi, A., Cardello, G.L., Petitta, M., 2021. Understanding the Origin and Mixing of Deep Fluids in Shallow Aquifers and Possible Implications for Crustal Deformation Studies: San Vittorino Plain, Central Apennines. Appl. Sci. 11 (4), 1353.

Barbieri, M., Boschetti, T., Barberio, M.D., Billi, A., Franchini, S., Iacumin, P., Selmo, E., Petitta, M., 2020. Tracing deep fluid source contribution to groundwater in an active seismic area (central Italy): A combined geothermometric and isotopic (δ13C) perspective. J. Hydrol. 582, 124495. https://doi.org/10.1016/j.jhydrol.2019.124495.

Barbieri, M., Franchini, S., Barberio, M. D., Billi, A., Boschetti, T., Giansante, L., Gori, F., Jónsson, S., Petitta, M., Skelton, A., Stockmann, G., 2021. Changes in groundwater trace element concentrations before seismic and volcanic activities in Iceland during 2010–2018. Sci. Total Environ. 148635.

Boncio, P., Dichiarante, A. M., Auciello, E., Saroli, M., Stoppa, F. 2016. Normal faulting along the western side of the Matese Mountains: Implications for active tectonics in the Central Apennines (Italy). J. Struct. Geol. 82, 16–36.

Boschetti, T., Barbieri, M., Barberio, M.D., Billi, A., Franchini, S., Petitta, M., 2019. CO_2 Inflow and Elements Desorption Prior to a Seismic Sequence, Amatrice-Norcia 2016, Italy. Geochem. Geophys. Geosyst. 20(5), 2303–2317. 10.1029/2018GC008117.

Bourg, A. C. M., Loch, J. G. 1995. Mobilization of heavy metals as affected by pH and redox conditions. In Biogeodynamics of pollutants in soils and sediments (pp. 87–102). Springer, Berlin, Heidelberg.

Bridgewater, L.L., Baird, R.B., Eaton, A.D., Rice, E.W., Association, A.P.H., Association, A.W.W., Federation, W.E. (Eds.), 2017. Standard methods for the examination of water and wasterwater, 23rd ed. American Public Health Association, Washington, DC.

Cardello, G.L., Mancktelow, N.S., 2015. Veining and post-nappe transtensional faulting in the SW Helvetic Alps (Switzerland). Swiss J. Geosci. 108 (2–3), 379–400.

Cardello, G.L., Vico, G., Consorti, L., Sabbatino, M., Carminati, E., Doglioni, C., 2021. Constraining the Passive to Active Margin Tectonics of the Internal Central Apennines: Insights from Biostratigraphy, Structural, and Seismic Analysis. Geosciences 11 (4), 160.

Cavinato, G.P., Celles, P.D., 1999. Extensional basins in the tectonically bimodal central Apennines fold-thrust belt, Italy: Response to corner flow above a subducting slab in retrograde motion. Geology 27 (10), 955–958.

Celico, F., Petrella, E., 2008. Evoluzione delle conoscenze idrogeologiche del settore nord-occidentale del massiccio carbonatico del Matese-nota preliminare. Mem. Descr. Carta Geol. d'Italia 77, 177–2182.

Chen, C.H., Tang, C.C., Cheng, K.C., Wang, C.H., Wen, S., Lin, C.H., Wen, Y.Y., Meng, G., Yeh, T.K., Jan, J.C., Yen, H.Y., Liu, J.Y., 2015. Groundwater–strain coupling before the 1999 Mw 7.6 Taiwan Chi-Chi earthquake. J. Hydrol. 524, 378–384. https://doi.org/10.1016/j.jhydrol.2015.03.006.

Chen, X., Jiang, C., Zheng, L., Zhang, L., Fu, X., Chen, S., Chen, Y., Hu, J., 2021. Evaluating the genesis and dominant processes of groundwater salinization by using hydrochemistry and multiple isotopes in a mining city. Environ. Pollut. 283, 117381.

Chiaraluce, L., Di Stefano, R., Tinti, E., Scognamiglio, L., Michele, M., Casarotti, E., Cattaneo, M., De Gori, P., Chiarabba, C., Monachesi, G., Lombardi, A., Valoroso, L., Latorre, D., Marzorati, S., 2017. The 2016 Central Italy Seismic Sequence: A First Look at the Mainshocks, Aftershocks, and Source Models. Seismo. Res. Lett. 88 (3), 757–771. https://doi.org/10.1785/0220160221.

Chiodini, G., Frondini, F., Cardellini, C., Parello, F., Peruzzi, L., 2000. Rate of diffuse carbon dioxide Earth degassing estimated from carbon balance of regional aquifers: The case of central Apennine, Italy. J. Geophys. Res. 105 (B4), 8423–8434. https://doi.org/10.1029/1999JB900355.

Chiodini, G., Cardellini, C., Amato, A., Boschi, E., Caliro, S., Frondini, F., Ventura, G., 2004. Carbon dioxide Earth degassing and seismogenesis in central and southern Italy. Geophys. Res. Lett. 31 (7), n/a–n/a.

Ciaccio, M. G., Improta, L., Marchetti, A., Nardi, A., BSI Working Group. 2021. The 2019-2020 repeated small swarms in the Benevento area, Southern Apennines, Italy. GNGTS 2021-39° Convegno Nazionale.

Claesson, L., Skelton, A., Graham, C., Dietl, C., Mörth, M., Torssander, P., Kockum, I., 2004. Hydrogeochemical changes before and after a major earthquake. Geology 32 (8), 641. https://doi.org/10.1130/G20542.110.1130/2004110.

Clark, I., 2015. Groundwater geochemistry and isotopes. CRC Press.

Coppola, M., Correale, A., Barberio, M.D., Billi, A., Cavallo, A., Fondriest, M., Nazzari, M., Paonita, A., Romano, C., Stagno, V., Viti, C., Vona, A., 2021. Meso-to nano-scale evidence of fluid-assisted co-seismic slip along the normal Mt. Morrone Fault, Italy: Implications for earthquake hydrogeochemical precursors. Earth Planet. Sci. Lett. 568, 117010. https://doi.org/10.1016/j.epsl.2021.117010.

Corniello, A., De Riso, R., 1986. Idrogeologia e idrochimica delle sorgenti dell'Agro Telesino (BN). Geologia applicata e Idrogeologia 21, 53–84.

Corniello, A., Guida, M., Stellato, L., Trifuoggi, M., Carraturo, F., Del Gaudio, E., Del Giudice, C., Forte, G., Giarra, A., Iorio, M., Marzaioli, F., Toscanesi, M., 2021. Hydrochemical, isotopic and microbiota characterization of telese mineral waters (Southern Italy). Environ. Geochem. Health. https://doi.org/10.1007/s10653-021-00806-4.

De Luca, G., Di Carlo, G., Tallini, M., 2018. A record of changes in the Gran Sasso groundwater before, during and after the 2016 Amatrice earthquake, central Italy. Sci. Rep. 8, 15982. https://doi.org/10.1038/s41598-018-34444-1.

Di Luccio, F., Chiodini, G., Caliro, S., Cardellini, C., Convertito, V., Pino, N.A., Tolomei, C., Ventura, G., 2018. Seismic signature of active intrusions in mountain chains. Sci. Adv. 4, e1701825. https://doi.org/10.1126/sciadv.1701825.

Doglioni, C., 1991. A proposal for the kinematic modelling of W-dipping subductions-possible applications to the Tyrrhenian-Apennines system. Terra Nova 3 (4), 423–434.

Doglioni, C., Harabaglia, P., Martinelli, G., Mongelli, F., Zito, G., 1996. A geodynamic model of the Southern Apennines accretionary prism. Terra Nova 8 (6), 540–547.

Doglioni, C., Barba, S., Carminati, E., Riguzzi, F., 2014. Fault on–off versus coseismic fluids reaction. Geosci. Front. 5 (6), 767–780. https://doi.org/10.1016/j.gsf.2013.08.004.

Doglioni, C., Carminati, E., Petricca, P., Riguzzi, F., 2015. Normal fault earthquakes or graviquakes. Sci. Rep. 5 (1), 1–12.

Drever, J. I. 2005. Surface and Ground Water, Weathering, and Soils: Treatise on Geochemistry, Volume 5 (Vol. 5). Elsevier.

Elkhoury, J.E., Brodsky, E.E., Agnew, D.C., 2006. Seismic waves increase permeability. Nature 441 (7097), 1135–1138. https://doi.org/10.1038/nature04798.

Fiorillo, F., Guadagno, F.M., 2010. Karst Spring Discharges Analysis in Relation to Drought Periods, Using the SPI. Water Resour. Manage. 24 (9), 1867–1884. https://doi.org/10.1007/s11269-009-9528-9.

Fiorillo, F., Pagnozzi, M., 2015. Recharge processes of Matese karst massif (southern Italy). Environ. Earth. Sci. 74 (12), 7557–7570. https://doi.org/10.1007/s12665-015-4678-y.

Fiorillo, F., Leone, G., Pagnozzi, M., Catani, V., Testa, G., Esposito, L., 2019. The Upwelling Groundwater Flow in the Karst Area of Grassano-Telese Springs (Southern Italy). Water 11, 872. https://doi.org/10.3390/w11050872.

Franchini, S., Agostini, S., Barberio, M.D., Barbieri, M., Billi, A., Boschetti, T., Pennisi, M., Petitta, M., 2021. HydroQuakes, central Apennines, Italy: Towards a hydrogeochemical monitoring network for seismic precursors and the hydro-seismo-sensitivity of boron. J. Hydrol. 598, 125754. https://doi.org/10.1016/j.jhydrol.2020.125754.

Frondini, F., Cardellini, C., Caliro, S., Beddini, G., Rosiello, A., Chiodini, G., 2019. Measuring and interpreting CO_2 fluxes at regional scale: the case of the Apennines, Italy. J. Geol. Soc. 176 (2), 408–416. https://doi.org/10.1144/jgs2017-169.

Galli, P., Galadini, F., Pantosti, D., 2008. Twenty years of paleoseismology in Italy. Earth-Sci. Rev. 88, 89–117. https://doi.org/10.1016/j.earscirev.2008.01.001.

Gutenberg, B., 1956. The energy of earthquakes. Quarter. J. Geol. Soc. 112 (1–4), 1–14.

Hosono, T., Masaki, Y., 2020. Post-seismic hydrochemical changes in regional groundwater flow systems in response to the 2016 Mw 7.0 Kumamoto earthquake. J. Hydrol. 580, 124340. https://doi.org/10.1016/j.jhydrol.2019.124340.

Hosono, T., Yamada, C., Manga, M., Wang, C.-Y., Tanimizu, M., 2020. Stable isotopes show that earthquakes enhance permeability and release water from mountains. Nat. Commun. 11, 2776. https://doi.org/10.1038/s41467-020-16604-y.

Hwang, H.S., Hamm, S.Y., Cheong, J.Y., Lee, S.H., Ha, K., Lee, C., Woo, N.C., Yun, S.M., Kim, K.H., 2020. Effective time-and frequency-domain techniques for interpreting seismic precursors in groundwater level fluctuations on Jeju Island. Korea. Sci. Rep. 10 (1), 1–14.

Igarashi, G., Saeki, S., Takahata, N., Sumikawa, K., Tasaka, S., Sasaki, Y., Takahashi, M., Sano, Y., 1995. Ground-Water Radon Anomaly Before the Kobe Earthquake in Japan. Science 269 (5220), 60–61. https://doi.org/10.1126/science:269.5220.60.

Inan, S., Balderer, W.P., Leuenberger-West, F., Yakan, H., Ozvan, A., Freund, F.T., 2012. Springwater chemical anomalies prior to the Mw = 7.2 Van eathquake (Turkey). Geochem. J. 46, 11–16.

Ingebritsen, S.E., Manga, M., 2014. Hydrogeochemical precursors. Nat. Geosci. 7 (10), 697–698.

Kawabata, K., Sato, T., Takahashi, H.A., Tsunomori, F., Hosono, T., Takahashi, M., Kitamura, Y., 2020. Changes in groundwater radon concentrations caused by the 2016 Kumamoto earthquake. J. Hydrol. 584, 124712.

Kim, J., Lee, J., Petitta, M., Kim, H., Kaown, D., Park, I.W., Lee, S., Lee, K.K., 2019. Groundwater system responses to the 2016 ML 5.8 Gyeongju earthquake. South Korea. J. Hydrol. 576, 150–163.

Kim, J., Joun, W. T., Lee, S., Kaown, D., Lee, K. K. 2020. Hydrogeochemical Evidence of Earthquake-Induced Anomalies in Response to the 2017 MW 5.5 Pohang Earthquake in Korea. Geochemistry, Geophys. Geosystems 21(12), e2020GC009532.

Lamberti, M.C., Vigide, N., Venturi, S., Agusto, M., Yagupsky, D., Winocur, D., Barcelona, H., Velez, M.L., Cardellini, C., Tassi, F., 2019. Structural architecture releasing deep-sourced carbon dioxide diffuse degassing at the Caviahue – Copahue Volcanic Complex. J. Volcanol. Geotherm. Res. 374, 131–141. https://doi.org/10.1016/j.jvolgeores.2019.02.004.

Lan, S., Gu, H., Yu-Liu, 2021. Changes in groundwater level and tidal response caused by the Wenchuan earthquake, China. Hydrogeol. J. 10.1007/s10040-021-02302-6.

Langmuir, D., 1997. Aqueous Environmental Geochemistry. Prentice-Hall, Inc., Upper Saddle River, NJ.

Lee, H. A., Hamm, S. Y., Woo, N. C. 2021. Pilot-Scale Groundwater Monitoring Network for Earthquake Surveillance and Forecasting Research in Korea. Water, 13(17), 2448.
Leone, G., Pagnozzi, M., Catani, V., Testa, G., Esposito, L., Fiorillo, F., 2019. Hydrogeology of the Karst Area of the Grassano and Telese Springs. AS-ITJGW. https://doi.org/10.7343/as-2019-415.
Li, B., Shi, Z., Wang, G., Liu, C., 2019. Xianshuihe Fault zone, Western China. J. Hydrol. 11.
Malakootian, M., Nouri, J., 2010. Chemical variations of ground water affected by the earthquake in bam region. Int. J. Environ. Res. 4 (3), 443–454.
Manahan, S.E., 2017. Environmental chemistry. CRC Press.
Manga, M., Wang, C.Y., 2015. Earthquake Hydrology. Treatise on. Geophysics 4, 25.
Martinelli, G., Ciolini, R., Facca, G., Fazio, F., Gherardi, F., Heinicke, J., Pierotti, L., 2021. Tectonic-Related Geochemical and Hydrological Anomalies in Italy during the Last Fifty Years. Minerals 11, 107. https://doi.org/10.3390/min11020107.
Mastrorillo, L., Saroli, M., Viaroli, S., Banzato, F., Valigi, D., Petitta, M., 2020. Sustained post-seismic effects on groundwater flow in fractured carbonate aquifers in Central Italy. Hydrol Process. 34 (5), 1167–1181.
Milano, G., Di Giovambattista, R., Ventura, G., 2006. Seismicity and stress field in the Sannio-Matese area. Ann. Geophys.
Minissale, A., 2004. Origin, transport and discharge of CO_2 in central Italy. Earth Sci. Rev. 66, 89–141.
Muir-Wood, R., King, G.C.P., 1993. Hydrological signatures of earthquake strain. J. Geophys. Res. 98 (B12), 22035–22068. https://doi.org/10.1029/93JB02219.
Nakagawa, K., Yu, Z.-Q., Berndtsson, R., Hosono, T., 2020. Temporal characteristics of groundwater chemistry affected by the 2016 Kumamoto earthquake using self-organizing maps. J. Hydrol. 582, 124519. https://doi.org/10.1016/j.jhydrol.2019.124519.
Onda, S., Sano, Y., Takahata, N., Kagoshima, T., Miyajima, T., Shibata, T., Pinti, D.L., Lan, T., Kim, N.K., Kusakabe, M., Nishio, Y., 2018. Groundwater oxygen isotope anomaly before the M6.6 Tottori earthquake in Southwest Japan. Sci. Rep. 8, 4800. https://doi.org/10.1038/s41598-018-23303-8.
Orihara, Y., Kamogawa, M., Nagao, T., 2014. Preseismic changes of the level and temperature of confined groundwater related to the 2011 Tohoku earthquake. Sci. Rep. 4 (1), 1–6.
Parkhurst, D. L., Appelo, C. A. J. 2013. Description of input and examples for PHREEQC version 3: a computer program for speciation, batch-reaction, one-dimensional transport, and inverse geochemical calculations (No. 6-A43). US Geological Survey.
Paudel, S.R., Banjara, S.P., Wagle, A., Freund, F.T., 2018. Earthquake chemical precursors in groundwater: a review. J. Seismol. 22 (5), 1293–1314. https://doi.org/10.1007/s10950-018-9739-8.
Pérez, N.M., Hernández, P.A., Padrón, E., Cartagena, R., Olmos, R., Barahona, F., Melián, G., Salazar, P., López, D.L., 2006. Anomalous diffuse CO_2 emission prior to the January 2002 short-term unrest at San Miguel Volcano, El Salvador, Central America. Pure Appl. Geophys. 163 (4), 883–896.
Petitta, M., Mastrorillo, L., Preziosi, E., Banzato, F., Barberio, M.D., Billi, A., Cambi, C., De Luca, G., Di Carlo, G., Di Curzio, D., Di Salvo, C., Nanni, T., Palpacelli, S., Rusi, S., Saroli, M., Tallini, M., Tazioli, A., Valigi, D., Vivalda, P., Doglioni, C., 2018. Water-table and discharge changes associated with the 2016–2017 seismic sequence in central Italy: hydrogeological data and a conceptual model for fractured carbonate aquifersChangements du niveau piézométrique et des débits associés à la séquence sismique 2016–2017 en Italie centrale: données hydrogéologiques et modèle conceptuel pour des aquifères carbonatés fracturésCambios en el nivel freático y en la descarga asociados con la secuencia sísmica 2016–2017 en el centro de Italia: datos hidrogeológicos y un modelo conceptual para acuíferos carbonatados fracturados意大利中部2016–2017年地震序列有关的水位和流量变化:水文地质数据和裂隙碳酸盐含水层的概念模型Mudanças no nível freático e na descarga associadas com a sequência sísmica 2016–2017 no centro da Itália: dados hidrológicos e um modelo conceitual para aquíferos carbonáticos fraturados. Hydrogeol. J. 26 (4), 1009–1026. https://doi.org/10.1007/s10040-017-1717-7.
Petrella, E., Celico, F., 2009. Heterogeneous aquitard properties in sedimentary successions in the Apennine chain: case studies in southern Italy. Hydrol. Process.: Int. J. 23 (23), 3365–3371.
Petricca, P., Barba, S., Carminati, E., Doglioni, C., Riguzzi, F., 2015. Graviquakes in Italy. Tectonophysics 656, 202–214.
Rajmohan, N., Elango, L.J.E.G., 2004. Identification and evolution of hydrogeochemical processes in the groundwater environment in an area of the Palar and Cheyyar River Basins, Southern India. Environ. Geol. 46 (1), 47–61.
Rufino, F., Cuoco, E., Busico, G., Caliro, S., Maletic, E.L., Avino, R., Darrah, T.H., Tedesco, D., 2021. Deep carbon degassing in the Matese massif chain (Southern Italy) inferred by geochemical and isotopic data. Environ. Sci. Pollut. Res. 28 (34), 46614–46626. https://doi.org/10.1007/s11356-020-11107-1.
Salazar, J.M.L., Pérez, N.M., Hernández, P.A., Soriano, T., Barahona, F., Olmos, R., Cartagena, R., López, D.L., Lima, N., Melián, G., Castro, L., Galindo, I., Notsu, K., 2002. Precursory diffuse carbon dioxide degassing signature related to a 5.1 magnitude earthquake in El Salvador, Central America. Earth Planet. Sci. Lett. 205 (1–2), 81–89.
Sano, Y., Takahata, N., Kagoshima, T., Shibata, T., Onoue, T., Zhao, D., 2016. Groundwater helium anomaly reflects strain change during the 2016 Kumamoto earthquake in Southwest Japan. Sci. Rep. 6, 37939. https://doi.org/10.1038/srep37939.
Shi, Z., Wang, G., Liu, C., 2013. Advances in research on earthquake fluids hydrogeology in China: a review. Earthq. Sci. 26 (6), 415–425.
Sibson, R.H., Moore, J.M.M., Rankin, A.H., 1975. Seismic pumping—a hydrothermal fluid transport mechanism. Journal of the Geological Society 131 (6), 653–659.
Sibson, R.H., 2000. Fluid involvement in normal faulting. J. Geodyn. 29 (3–5), 469–499.
Silverii, F., 2016. Study of the transient deformation of Central and Southern Apennines from GPS observations. Doctoral. Dissertation.
Skelton, A., Andrén, M., Kristmannsdóttir, H., Stockmann, G., Mörth, C.-M., Sveinbjörnsdóttir, Á., Jónsson, S., Sturkell, E., Guðrúnardóttir, H.R., Hjartarson, H., Siegmund, H., Kockum, I., 2014. Changes in groundwater chemistry before two consecutive earthquakes in Iceland. Nat. Geosci. 7 (10), 752–756. https://doi.org/10.1038/ngeo2250.
Skelton, A., Liljedahl-Claesson, L., Wästeby, N., Andrén, M., Stockmann, G., Sturkell, E., Mörth, C.-M., Stefansson, A., Tollefsen, E., Siegmund, H., Keller, N., Kjartansdóttir, R., Hjartarson, H., Kockum, I., 2019. Hydrochemical Changes Before and After Earthquakes Based on Long-Term Measurements of Multiple Parameters at Two Sites in Northern Iceland—A Review. J. Geophys. Res. Solid Earth 124 (3), 2702–2720. https://doi.org/10.1029/2018JB016757.
Tamburello, G., Pondrelli, S., Chiodini, G., Rouwet, D., 2018. Global-scale control of extensional tectonics on CO_2 earth degassing. Nat. Commun. 9 (1), 1–9.
Tsunogai, U., Wakita, H., 1995. Precursory chemical changes in ground water: Kobe earthquake, Japan. Science 269 (5220), 61–63.
Tullis, J., Yund, R., Farver, J., 1996. Deformation-enhanced fluid distribution in feldspar aggregates and implications for ductile shear zones. Geology 24 (1), 63–66.
Wakita, H., 1975. Water Wells as Possible Indicators of Tectonic Strain. Science 189 (4202), 553–555. https://doi.org/10.1126/science:189.4202.553.
Wakita, H., Nakamura, Y., Notsu, K., Noguchi, M., Asada, T., 1980. Radon anomaly: a possible precursor of the 1978 Izu-Oshima-kinkai earthquake. Science 207 (4433), 882–883.
Wang, C.Y., Wang, L.P., Manga, M., Wang, C.H., Chen, C.H., 2013. Basin-scale transport of heat and fluid induced by earthquakes. Geophys. Res. Lett. 40 (15), 3893–3897.
Wang, C.Y., Manga, M., 2021. Water and Earthquakes. Springer Nature.
Wannamaker, P.E., Jiracek, G.R., Stodt, J.A., Caldwell, T.G., Gonzalez, V.M., McKnight, J.D., Porter, A.D., 2002. Fluid generation and pathways beneath an active compressional orogen, the New Zealand Southern Alps, inferred from magnetotelluric data. J. Geophys. Res. Solid Earth 107 (B6), ETG-6.
Wästeby, N., Skelton, A., Tollefsen, E., Andrén, M., Stockmann, G., Claesson Liljedahl, L., Sturkell, E., Mörth, M., 2014. Hydrochemical monitoring, petrological observation, and geochemical modeling of fault healing after an earthquake: Fault healing after an earthquake. J. Geophys. Res. Solid Earth 119 (7), 5727–5740. https://doi.org/10.1002/2013JB010715.